

Report Number 10/21

**CARDIAC ELECTROMECHANICS: THE EFFECT OF
CONTRACTION MODEL ON THE MATHEMATICAL
PROBLEM AND ACCURACY OF THE NUMERICAL SCHEME**

by

P. Pathmanathan, S. J. Chapman, D. J. Gavaghan, J. P. Whiteley



Oxford Centre for Collaborative Applied Mathematics
Mathematical Institute
24 - 29 St Giles'
Oxford
OX1 3LB
England

CARDIAC ELECTROMECHANICS: THE EFFECT OF CONTRACTION MODEL ON THE MATHEMATICAL PROBLEM AND ACCURACY OF THE NUMERICAL SCHEME

by P. Pathmanathan

(University of Oxford, Computing Laboratory, Wolfson Building, Parks Road, Oxford, OX1 3QD, UK, pras@comlab.ox.ac.uk, Tel: +44 1865 273838, Fax: +44 1865 273839)

S. J. Chapman

(University of Oxford, Mathematical Institute, 24-29 St Giles, Oxford, OX1 3LB, UK, chapman@maths.ox.ac.uk)

D. J. Gavaghan

(University of Oxford, Computing Laboratory, Wolfson Building, Parks Road, Oxford, OX1 3QD, UK, gavaghan@comlab.ox.ac.uk)

J. P. Whiteley

(University of Oxford, Computing Laboratory, Wolfson Building, Parks Road, Oxford, OX1 3QD, UK, jonathan.whiteley@comlab.ox.ac.uk)

[Received ???. Revise ???]

Summary

Models of cardiac electromechanics usually contain a contraction model determining the active tension induced at the cellular level, and the equations of nonlinear elasticity to determine tissue deformation in response to this active tension. All contraction models are dependent on cardiac electro-physiology, but can also be dependent on the stretch and stretch-rate in the fibre direction. This fundamentally affects the mathematical problem being solved, through classification of the governing PDEs, which affects numerical schemes that can be used to solve the governing equations. We categorise contraction models into three types, and for each consider questions such as classification and the most appropriate choice from two numerical methods (the explicit and implicit schemes). In terms of mathematical classification, we consider the question of strong ellipticity of the total strain energy (important for precluding ‘unnatural’ material behaviour) for stretch-rate-independent contraction models; whereas for stretch-rate-dependent contraction models we introduce a corresponding third-order problem and explain how certain choices of boundary condition could lead to constraints on allowable initial condition. In terms of suitable numerical methods, we show that an explicit approach (where the contraction model is integrated in the timestep prior to the bulk deformation being computed) is: (i) appropriate for stretch-independent contraction models; (ii) only conditionally-stable, with the stability criterion independent of timestep, for contractions models which just depend on stretch (but not stretch-rate), and (iii) inappropriate for stretch-rate-dependent models.

1. Introduction

Mathematical modelling of cardiac activity is a significant tool in understanding the mechanisms behind healthy and aberrant cardiac behaviour, and the inclusion of the mechanical activity in tissue is an important aspect of such modelling. Most models of cardiac electromechanics comprise four components. The first two are the partial differential equations (PDEs) and ordinary differential equations (ODEs) of the electrophysiological model. The third component is the cellular *contraction model*, a set of ODEs at each point in space which determine the active tension induced in a single cell resulting from electrical activation. This paper is restricted to such ‘weakly-coupled’ models, in which the contraction model is considered separately to the cell model, although ‘strongly-coupled’ approaches can also be taken: we discuss later how the results of this paper transfer to strongly coupled models. The fourth component is the PDEs of incompressible nonlinear elasticity, which are dependent on the active tension. The contraction model can be also dependent on the deformation, through the stretch in the cardiac fibre direction, and possibly also through the stretch-rate. The key observation is that this fundamentally affects the form of the PDEs of nonlinear elasticity, and therefore affects both their mathematical properties and the appropriate choice of numerical solution procedure.

For example, if the contraction model depends on stretch-rate, the nonlinear elasticity problem is, as shall be explained, a *third-order* problem. Even if the contraction model does not depend on stretch-rate, the dependence on the active tension can affect the *strong ellipticity* of the strain energy function, i.e. the ellipticity of the nonlinear elasticity problem. The existence of singular solutions (1), or those corresponding to discontinuous deformation gradients (2), or those with other undesirable properties, can be attributed to a loss of ellipticity of the governing equations (3), and strong ellipticity of the material law is an important property to establish so that such behaviour can be precluded. Furthermore, ellipticity ensures the absence of certain types of non-physical singularity which can lead to serious numerical problems (4), so ellipticity is also extremely desirable from a computational point of view. As far as we are aware, establishing the ellipticity of problems of *active* cardiac electromechanics has not previously been investigated, although work (4, 2) has been done determining conditions for ellipticity of passive cardiac material laws.

There are two numerical solution approaches which we consider: the *explicit* approach, which involves solving the contraction models prior to computing the bulk deformation, and has been commonly used in cardiac electromechanical simulations; and the *implicit* method described in (5), which was developed as a stable numerical scheme for electromechanics following observations (6, 7) of the numerically unstable behaviour of the explicit method.

This paper is concerned with the effect of the choice of contraction model on the mathematical formulation of cardiac electromechanical problems and the numerical solution procedure. We categorise the contraction model into three types, based on whether the contraction model depends on: (i) neither fibre-stretch nor fibre-stretch-rate; (ii) just fibre-stretch; or (iii) both fibre-stretch and fibre-stretch-rate. For each category, we investigate which type of numerical method is appropriate, and consider ellipticity of the resultant PDEs (establishing conditions on the passive part of the strain energy for ellipticity to hold), or undergo a general mathematical analysis of the equations.

We begin in Section 2 by fully describing the components of cardiac electromechanical

models and the three categories of contraction model. The explicit and implicit methods are then outlined in Section 3. In Section 4 we study the case where the contraction model just depends on the electrophysiology, and not the deformation, stating the appropriate choice of method (the explicit scheme) and investigating strong ellipticity of the problem.

The situation where the contraction model depends on the fibre-stretch is more complicated, and studied in Section 5. Here, we explain why the explicit scheme is only conditionally stable, with the stability criterion dependent on the spatial stepsize but not the timestep, so that stability cannot be gained, as is common with other problems, by reducing the timestep.

Finally, in Section 6, we look at the stretch- and stretch-rate-dependent case. We explain why the explicit method fails in this case as a simple bad time-discretisation—not, as previously held, as the explicit method being an unstable scheme (in the traditional numerical analysis sense of the term). We also investigate a third-order PDE which arises from this problem. We will show how in this case the role of boundary conditions can have a subtle but significant effect on allowable initial conditions.

2. Components of cardiac electromechanical problems

As commonly implemented, there are four main components of models of cardiac electromechanics. These are illustrated in Fig. 1. The first two components together form the electrophysiological model—either the monodomain equations or the bidomain equations. The first component is the PDE (or two coupled PDEs in the bidomain case) representing propagation through the tissue of the electrical current, which is modelled by a reaction-diffusion equation for the transmembrane voltage, V , (or voltage and extracellular potential in the bidomain case). This is coupled to the second component, a set of ODEs—the *cell model*—which determine how individual cells become electrically activated. These ODEs have as state variables cell-level quantities (which we denote by \mathbf{u}) such as ionic concentrations and probabilities of membrane ion channels being open. They are coupled to the first component by being dependent on the transmembrane voltage, but providing the ionic current which acts as the source term in the reaction-diffusion PDEs.

In electrophysiological problems in which the mechanical deformation is neglected, the monodomain equations take the form

$$\chi C_m \frac{\partial V}{\partial t} = \nabla \cdot (\sigma \nabla V) - \chi I_{\text{ion}}(\mathbf{u}, V), \quad (2.1)$$

$$\frac{d\mathbf{u}}{dt} = \mathbf{f}(\mathbf{u}, V), \quad (2.2)$$

(we will describe shortly how these equations are modified to take the deformation into account), where χ is the surface-area-to-volume-ratio of a cardiac cell, C_m the capacitance across the cell membrane, σ the conductivity of the tissue, I_{ion} the ionic current, and \mathbf{f} a general function representing the choice of cell-model. A large number of cell-models have been proposed in the literature, with ever-increasing physiological complexity exhibiting itself through ever-increasing numbers of state variables, examples of which can be found in the ‘CellML’ repository (<http://www.cellml.org/>). For a description of the bidomain equations see (8).

The third component of cardiac electromechanical problems is the cell-level contraction

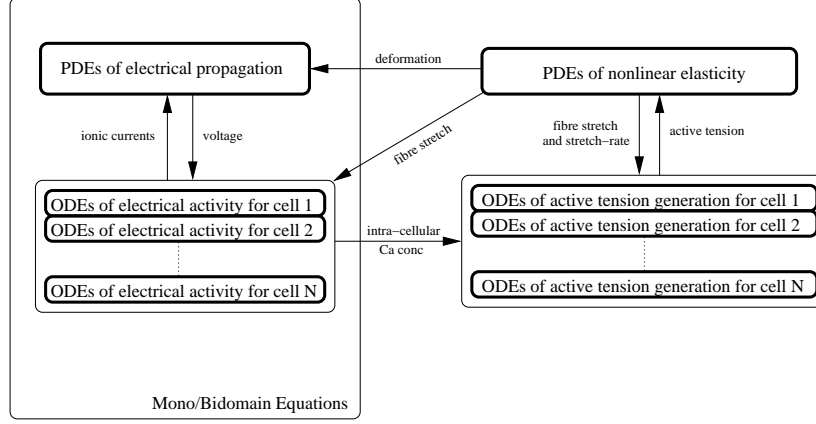


Fig. 1 Components of cardiac electromechanical models.

model, which determines the *active tension* generated in response to electrical activation of a single cell. These are typically modelled using ODEs, usually in far fewer variables than the cell model, and generally provide the active tension, σ_a , induced in the cell[†]. We have written σ_a rather than the more common T_a to denote the active tension as we assume the active tension is a true (Cauchy) stress, not a transformed stress. The type of stress that the active tension is depends on the protocol of the experiments that have been used for fitting contraction model parameters. If the deformed cross-sectional area is measured along with the force, the experimental stress will be a Cauchy stress. However, some protocols may have used the undeformed cross-sectional area, in which case the experimental stress, and therefore the active tension provided by the model, will be a first Piola-Kirchoff (9) stress (for example, the contraction model used in (10)).

Physiologically, the mechanical response in the cell is dependent on the electrical activity largely through the intracellular calcium concentration, $[\text{Ca}^{2+}]$, and therefore most contraction models take this as input, although some simpler models are instead dependent on the voltage and some also explicitly on time. The contraction model can also be dependent on the fibre-stretch (the stretch ratio in the fibre direction), λ , as well as possibly on the fibre-stretch-rate, $\dot{\lambda}$, and it is this dependency that is the focus of this paper. Let \mathbf{w} be a vector of internal state variables for the contraction model. We write the model in its most general form as

$$\frac{d\mathbf{w}}{dt} = \mathbf{g}(\mathbf{w}, t; [\text{Ca}^{2+}], V, \lambda, \dot{\lambda}), \quad (2.3)$$

$$\sigma_a \equiv \sigma_a(\mathbf{w}, t; [\text{Ca}^{2+}], V, \lambda, \dot{\lambda}). \quad (2.4)$$

Note that in describing the components of cardiac electromechanical models in this way,

[†] Note that the phrase ‘active tension’ is a misnomer—this is actually a stress. We retain the commonly-used phrase ‘active tension’, and throughout this paper ‘active tension’ will refer to this scalar, cell-level, stress induced in this cell, σ_a ; and ‘active stress’ will refer to the full, tensor, active part of the stress, which will be denoted by T^{active} or σ^{active} .

we are restricting ourselves to *weakly coupled models*, in which the contraction model is considered separate to the cell model. An alternative approach involves the use of a single, larger, system of ODEs to model the electrical activity and contraction at the cell level together. Consideration of such *strongly-coupled models* is outside the scope of this paper. However this is only because the implementation of the implicit method (to be discussed in the next section) will be more complicated for such models—the analysis will still hold for strongly-coupled models, as will be discussed in Section 7. The manner in which the active tension is dependent on the electro-physiology has no effect on the results in this paper.

The final component is the model of tissue deformation. In common with other authors we assume that cardiac tissue can be modelled as a nonlinear, incompressible, hyperelastic solid, in which case this component takes the form of the PDEs of nonlinear elasticity (9). Let $\Omega_0 \subset \mathbb{R}^3$ denote a body in its undeformed, stress-free configuration, let \mathbf{X} be a point in Ω_0 , and let \mathbf{x} be the corresponding point in a deformed configuration, Ω , under some given loads. The deformation gradient is defined to be $F = \frac{\partial \mathbf{x}}{\partial \mathbf{X}}$, and the Green deformation tensor is $C = F^T F$. The stretch in the fibre direction is then $\lambda = \sqrt{\mathbf{m}^T C \mathbf{m}}$, where \mathbf{m} is the (undeformed) unit fibre direction. The 2nd Piola-Kirchhoff stress (9), T , is related to the deformation through a material-dependent strain energy function $W(C)$ such that the passive response of the material is given by $T^{\text{passive}} = 2 \frac{\partial W}{\partial C} - pC^{-1}$, where p is the pressure in the body (a Lagrange multiplier resulting from the constraint of incompressibility which has to be solved for together with the deformation). In standard elasticity problems $T = T^{\text{passive}}$. Assuming (6) that the tissue is always instantaneously in equilibrium and that that inertial effects can be neglected (i.e. quasi-steady), and neglecting the effect of gravity, the equation of equilibrium are:

$$\frac{\partial}{\partial X_M} (T_{MN} F_{iN}) = 0, \quad i = 1, 2, 3, \quad (2.5)$$

$$\det(F) = 1. \quad (2.6)$$

Suitable boundary conditions are the specification of the displacement in one region of the boundary of Ω_0 and surface traction on the remainder of the boundary.

These standard equations of nonlinear elasticity are amended to take into account the active response of the tissue by introducing a third term to the stress which depends on the active tension

$$T = 2 \frac{\partial W}{\partial C} - pC^{-1} + \frac{\sigma_a}{\mathbf{m}^T C \mathbf{m}} \mathbf{m} \mathbf{m}^T, \quad (2.7)$$

or

$$T = T^{\text{passive}} + T^{\text{active}}, \quad (2.8)$$

where

$$T^{\text{active}} = \frac{\sigma_a}{\lambda^2} \mathbf{m} \mathbf{m}^T. \quad (2.9)$$

T^{active} is the active (tensor) stress corresponding to the cellular active tension that is induced in the fibre direction. The denominator just scales the active tension for the undeformed state (the 2nd Piola-Kirchhoff tensor being a measure of stress that has been transformed to the undeformed state). This was derived in (5) using eigenvalues of stress, but there is a much simpler derivation: the Cauchy active (tensor) stress is $\sigma^{\text{active}} = \sigma_a \tilde{\mathbf{m}} \tilde{\mathbf{m}}^T$, where

$\tilde{\mathbf{m}} = F\mathbf{m}/\|F\mathbf{m}\|$ is the deformed unit fibre direction. The second Piola-Kirchhoff stress obeys $T = (\det F)^{-1}F^{-1}\sigma F^{-T}$, so (using $\det F = 1$ by incompressibility)

$$T^{\text{active}} = \frac{\sigma_a F^{-1} F\mathbf{m}(F\mathbf{m})^T F^{-T}}{\|F\mathbf{m}\|^2} = \frac{\sigma_a \mathbf{m}\mathbf{m}^T}{\mathbf{m}^T C \mathbf{m}}.$$

Similarly, if instead the contraction model provided a first Piola-Kirchhoff stress, s_a say, the tensor first Piola-Kirchhoff stress would be $S_{M_i}^{\text{active}} = s_a m_M \tilde{m}_i$ and we would have $T^{\text{active}} = S^{\text{active}} F^{-T} = s_a \mathbf{m}\mathbf{m}^T / \|F\mathbf{m}\|$, i.e. $T^{\text{active}} = s_a \mathbf{m}\mathbf{m}^T / \lambda$. If the contraction model provides a 2nd Piola-Kirchhoff stress t_a , then $T^{\text{active}} = t_a \mathbf{m}\mathbf{m}^T$.

This paper is restricted to such models of active cardiac mechanics in which the cellular active tension is determined and contributes additively to the total stress. An interesting alternative approach, related the theories of nonlinear plasticity and nonlinear tissue growth, involves multiplicatively decomposing the deformation gradient into an elastic part and an active part, $F = F_e F_a$, and solving the equilibrium equation (2.5) with $T = T(F_e) = T(F F_a^{-1})$ (11, 12). Such models, however, are beyond the scope of this paper.

Finally, the deformation affects the electrical activity in two ways, firstly, by changing the geometry over which the voltage propagates, affecting spatial derivatives in (2.1); and secondly, altering the cellular dynamics through mechano-electric feedback (MEF), and in particular the activation of stretch-activated ion channels in the cell membrane. A detailed description of MEF can be found in (13). Taking the cellular dynamics to be dependent on axial stretch only (although, in more generality, it could also be dependent on volume changes (14) and strain rates (15)), equations (2.1) and (2.2) become

$$\chi C_m \frac{\partial V}{\partial t} = \nabla \cdot (F^{-1} \sigma F^{-T} \nabla V) - \chi I_{\text{ion}}(\mathbf{u}, V, \lambda), \quad (2.10)$$

$$\frac{d\mathbf{u}}{dt} = \mathbf{f}(\mathbf{u}, V, \lambda). \quad (2.11)$$

In this paper, we neglect both these effects (in other words, use (2.1) and (2.2) instead of (2.10) and (2.11)). Firstly, we assume stretch-independent cellular dynamics. The changes to the spatial derivatives are neglected since it was shown in (5) that, in the isotropic σ case (the case for the simulations in this paper), for which $F^{-1} \sigma F^{-T} = C^{-1} \sigma$, replacing the C^{-1} with the identity tensor introduces very little error in the deformation in the case of simple propagation. The numerical experiments supporting the analysis in this paper therefore do not take into account any of the coupling back of the deformation on the electrophysiology. However, following numerical experiments in (5), it is not expected that including this coupling will introduce additional numerical problems.

Many contraction models have been proposed in the literature, although far fewer than there are cell-models. Some just relate the active tension to the electrophysiology through algebraic relationships (for example, (10, 16)), but most are ODE-based, and range from simple, phenomenological models, such as (17) or (18) which both just depend on the voltage (and time) and use a single ODE in which the state variable is the active tension; to physiological contraction models such as (19) which depends on the fibre stretch and also has a single ODE, this time in the length of the cellular contractile element, or the ‘NHS’ contraction (20) (modified in (7)) which contains a system of five ODEs. We classify the models based on their dependency on deformation. As we are concerned

with the dependency on the deformation, we will write, for example, $\sigma_a([\text{Ca}^{2+}])$ instead of $\sigma_a([\text{Ca}^{2+}], V, t)$, and for clarity sometimes write, for example, $\sigma_a(\lambda)$ instead of $\sigma_a([\text{Ca}^{2+}], \lambda)$ leaving the $[\text{Ca}^{2+}]$ dependence implicit. There are three categories:

1. Contraction model just dependent on electro-physiological variables (for example, (21, 17, 18)), i.e. $\sigma_a \equiv \sigma_a([\text{Ca}^{2+}])$
2. Contraction model also dependent on the fibre-stretch (for example, (16, 19, 10, 22, 23)), i.e. $\sigma_a \equiv \sigma_a([\text{Ca}^{2+}], \lambda)$
3. Contraction model also dependent on the fibre-stretch and fibre-stretch-rate (for example, (24, 20)), i.e. $\sigma_a \equiv \sigma_a([\text{Ca}^{2+}], \lambda, \dot{\lambda})$

The important observation is that the active tension being dependent on the deformation affects the classification of the equilibrium equation (2.5). In the standard elasticity problem T is just the passive material response, T^{passive} , which is a function of the first-derivatives of \mathbf{x} . In this case (2.5) contains second-derivatives of \mathbf{x} (i.e. is second-order), and is well-known to be elliptic (for appropriate choices of W). However, in cardiac electromechanics $T = T^{\text{passive}} + T^{\text{active}}$. Noting that λ is a function of the first spatial derivatives of deformation, we have three possibilities:

1. $\sigma_a([\text{Ca}^{2+}])$ is independent of \mathbf{x} , so $T^{\text{active}} = \frac{\sigma_a}{\lambda^2} \mathbf{m} \mathbf{m}^T$ is dependent on first-derivatives of \mathbf{x} in a specific way. The equilibrium PDE (2.5) is second-order but not necessarily elliptic.
2. $\sigma_a([\text{Ca}^{2+}], \lambda)$ dependent on \mathbf{x} , so T^{active} is a function of the first-derivatives of \mathbf{x} in a contraction-model-dependent way. The equilibrium PDE (2.5) is second-order but not necessarily elliptic.
3. $\sigma_a([\text{Ca}^{2+}], \lambda, \dot{\lambda})$ dependent on second-derivatives of \mathbf{x} , which are mixed derivatives (for example, $\frac{\partial^2 \mathbf{x}}{\partial X_M \partial t}$). The equilibrium PDE (2.5) is *third-order* and standard classification as elliptic/hyperbolic does not apply.

Note that due to σ_a being a Cauchy stress, even if σ_a is independent of λ , T^{active} will still be deformation-dependent.

3. The explicit and implicit methods

There are two types of algorithm for computing the numerical solution of cardiac electromechanical problems, which we shall refer to as the *explicit algorithm* and the *implicit algorithm*. The explicit algorithm is a common method for solving such problems as it is (relatively) computationally inexpensive and less difficult to implement. It involves computing the solution of the electrophysiological part of the model first (which is also the case for the implicit method), then solving the contraction models, then updating the deformation. The explicit approach or some variant of it has been used in (25, 17) and presumably in most of the (many) related works which do not specifically state full details of their numerical procedure. In more detail, the explicit algorithm is:

- Given the current voltage and deformation, on each timestep:
 - Solve the mono- or bidomain equations using any appropriate numerical scheme.
 - Pass $[\text{Ca}^{2+}]$ or V from the cell-model to the contraction model.
 - If the contraction model depends on λ or $\dot{\lambda}$, use the current deformation to calculate these and pass them to the contraction model.

- Integrate the contraction model ODEs to obtain the active tension σ_a at each point in space.
- Using this σ_a solve the PDEs of nonlinear elasticity for the new deformation.
- Repeat until the final time is reached.

The explicit algorithm can be visualised using Fig. 1, with the arrows representing information passed from one timestep to the next.

The explicit method has been observed to be unstable in certain situations (6, 7), and the implicit method used in this study was proposed in (5) as a stable algorithm for cardiac electromechanics. Essentially it involves embedding the contraction models in the PDEs of nonlinear elasticity, as illustrated in Fig. 2, by solving the contraction models together with the deformation. The explicit approach decouples these two components, whereas the implicit method computes them together, at a considerable loss in computational efficiency[†]. In more detail, the implicit algorithm is:

- Given the current voltage and deformation, on each timestep:
 - Solve the mono- or bidomain equations using any appropriate numerical scheme.
 - Pass $[\text{Ca}^{2+}]$ or V from the cell-model to the contraction model.
 - Solve the contraction model ODEs and the PDEs of nonlinear elasticity *at the same time*. Whenever a stress, $T \equiv T(\mathbf{x})$, has to be evaluated:
 - Compute λ and $\dot{\lambda}$ from \mathbf{x}
 - Integrate the contraction model ODEs using this λ and $\dot{\lambda}$, to obtain σ_a
 - Compute T using this σ_a .
- Repeat, until the final time is reached.

The difference between the two methods is made more clear by writing the stress as a function of the deformation at the current and previous timesteps. Suppose, at time t^n , we have computed the voltage V^n and deformation \mathbf{x}^n . In both methods we then solve the monodomain/bidomain equations to obtain the V^{n+1} . Let C^n denote $C(\mathbf{x}^n)$, λ^n denote $\lambda(\mathbf{x}^n)$, etc. To compute the deformation, we solve (2.5), using, in the explicit method, the following relationship between stress and deformation:

$$T = 2 \frac{\partial W}{\partial C}(C^{n+1}) - p(C^{n+1})^{-1} + \frac{\sigma_a(\lambda^n, \dot{\lambda}^n)}{(\lambda^{n+1})^2} \mathbf{m} \mathbf{m}^T, \quad (3.1)$$

whereas the implicit method uses

$$T = 2 \frac{\partial W}{\partial C}(C^{n+1}) - p(C^{n+1})^{-1} + \frac{\sigma_a(\lambda^{n+1}, \dot{\lambda}^{n+1})}{(\lambda^{n+1})^2} \mathbf{m} \mathbf{m}^T, \quad (3.2)$$

which leads to the contraction models being re-integrated whenever the stresses are evaluated. More details on the implicit method can be found in (5). A related method,

[†] The implicit scheme, when the same timesteps and ODE solvers are used as the explicit scheme, must be less efficient, since it involves calculating the active tensions many times per timestep when the explicit scheme just calculates them once. However, for the stretch-dependent cases, the implicit method can allow larger timesteps to be used, and with careful implicit ODE solving, the implicit scheme can be overall a more efficient choice of algorithm.

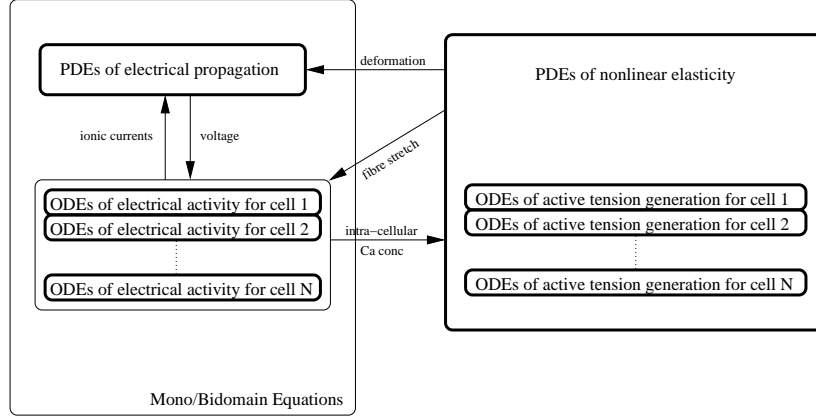


Fig. 2 Schematic of the implicit algorithm.

specific to the NHS contraction model (20)[‡] and in which selected parts of the contraction model are treated implicitly in order to obtain a stable scheme, is described in (7).

We use the finite element method (26) to solve both sets of PDEs for all the calculations in this paper. The electrophysiology is solved using a triangular mesh with linear basis functions to interpolate the voltage, and the mechanics is computed on a separate (coarser (5)) triangular mesh with quadratic bases for position and linear bases for pressure. The large nonlinear system arising from the finite element discretisation of the equations (27) is solved using Newton's method with damping.

4. Stretch- and stretch-rate-independent contraction models: $\sigma_a \equiv \sigma_a([\text{Ca}^{2+}])$ only

4.1 Choice of scheme

Looking at (2.7), at first glance the case where the contraction model is not dependent on λ and $\dot{\lambda}$ does not seem particularly different to the case where the contraction model is dependent on just λ (not $\dot{\lambda}$), since in both these two cases the active part of the second Piola-Kirchhoff stress, T^{active} , is dependent on λ . This is not the case, however. We can say without numerical analysis or numerical investigation that, unlike the latter case, the explicit method should certainly be used when the contraction model is completely independent of stretch and stretch-rate. This is because both methods would give identical results (and the implicit method far less efficiently), which is clear given the equivalence of (3.1) and (3.2) when σ_a is independent of λ and $\dot{\lambda}$. Of course, this is because it is only any stretch-dependence in σ_a that is treated explicitly (evaluated at the previous timestep) in the explicit method (as we have described it), not the whole of T^{active} .

[‡] This can be contrasted to the implicit algorithm described above, which can be applied to any contraction model. The techniques which make it efficient, however, (outlined in (5)) were specific to the NHS contraction model.

4.2 Conditions for strong ellipticity

For this type of contraction model, the known dependence of λ in the active stress renders it amenable to mathematical analysis. Let us denote λ^2 as I_4 , as is standard in problems of transverse isotropy, so that $I_4 \equiv \mathbf{m}^T C \mathbf{m} \equiv \|F \mathbf{m}\|^2 \equiv \lambda^2$. The active stress is $T^{\text{active}} = \frac{\sigma_a}{I_4} \mathbf{m} \mathbf{m}^T$. This can in fact be integrated to obtain a corresponding strain energy: let

$$W^{\text{active}} = \frac{1}{2} \sigma_a \log(I_4),$$

then, using the fact that σ_a is independent of \mathbf{x} , $2 \frac{\partial W^{\text{active}}}{\partial C} = \frac{\sigma_a}{I_4} \mathbf{m} \mathbf{m}^T = T^{\text{active}}$. Therefore we can write the *total* strain energy as $W^{\text{total}} = W^{\text{passive}} + W^{\text{incomp}} + W^{\text{active}}$, where W^{passive} is the strain energy for the passive material response and $W^{\text{incomp}} = -\frac{1}{2} p (\det(C) - 1)$ is the material-independent part of the strain energy arising from the constraint of incompressibility.

We would like to be able to say that, for any elliptic passive strain energy, the total strain energy is also elliptic, i.e. that the active strain energy does not affect the ellipticity properties of the total energy. Unfortunately, however, this is not the case. Instead, we show below that the active strain energy *cannot* be considered in isolation of the passive energy—rather, the ellipticity or lack of ellipticity of problems of cardiac electromechanics can only be determined in conjunction with a specific choice of passive strain energy.

A *compressible* strain-energy is strongly-elliptic (28) at a deformation gradient F_0 if

$$\frac{\partial^2 W}{\partial F_{iM} \partial F_{jN}} a_i a_j b_M b_N > 0 \quad \text{at } F = F_0 \quad \forall \mathbf{a} \neq 0, \mathbf{b} \neq 0. \quad (4.1)$$

It is strongly elliptic if (4.1) holds for all deformation gradients F_0 . Henceforth we write F instead of F_0 and assume the difference between derivatives with respect to F and evaluation at $F = F_0$ is understood. For *incompressible* strain energies, the test tensors are restricted but W^{incomp} does not need to be considered: let $\hat{W} = W - W^{\text{incomp}}$ (i.e. $W^{\text{passive}} + W^{\text{active}}$), then the condition for strong ellipticity is (28):

$$\frac{\partial^2 \hat{W}}{\partial F_{iM} \partial F_{jN}} a_i a_j b_M b_N > 0 \quad \forall \mathbf{a} \neq 0, \mathbf{b} \neq 0 : F_{Mi}^{-1} a_i b_M = 0. \quad (4.2)$$

Suppose W^{passive} is strongly elliptic—i.e. satisfies (4.2)—and $\sigma_a > 0$. The total strain energy will be strongly-elliptic for any choice of strongly-elliptic passive energy if

$$\frac{\partial^2 W^{\text{active}}}{\partial F_{iM} \partial F_{jN}} a_i a_j b_M b_N \geq 0 \quad \forall \mathbf{a}, \mathbf{b} : F_{Mi}^{-1} a_i b_M = 0. \quad (4.3)$$

Now, $\frac{\partial W^{\text{active}}}{\partial F_{iM}} = \frac{\sigma_a}{I_4} F_{iP} m_P m_M$, so

$$\frac{\partial^2 W^{\text{active}}}{\partial F_{iM} \partial F_{jN}} = -\frac{2\sigma_a}{I_4^2} F_{iP} m_P m_M F_{jQ} m_Q m_N + \frac{\sigma_a}{I_4} \delta_{ij} m_M m_N,$$

and therefore

$$\begin{aligned} \frac{\partial^2 W^{\text{active}}}{\partial F_{iM} \partial F_{jN}} a_i a_j b_M b_N &= -\frac{2\sigma_a}{I_4^2} ((F \mathbf{m}) \cdot \mathbf{a})^2 (\mathbf{b} \cdot \mathbf{m})^2 + \frac{\sigma_a}{I_4} (\mathbf{a} \cdot \mathbf{a})^2 (\mathbf{b} \cdot \mathbf{m})^2 \\ &= \frac{\sigma_a (\mathbf{b} \cdot \mathbf{m})^2}{I_4^2} \left(\|\mathbf{a}\|^2 I_4 - 2 ((F \mathbf{m}) \cdot \mathbf{a})^2 \right). \end{aligned} \quad (4.4)$$

To show that this quantity can be negative consider $\mathbf{a} = F\mathbf{m}$. Then $\|\mathbf{a}\|^2 I_4 - 2((F\mathbf{m}) \cdot \mathbf{a})^2 = -\|F\mathbf{m}\|^4 < 0$. However \mathbf{a} and \mathbf{b} must satisfy $F_{Mi}^{-1} a_i b_M = 0$ which means that $\mathbf{b} \cdot \mathbf{m} = 0$ and it follows that $\frac{\partial^2 W^{\text{active}}}{\partial F_{iM} \partial F_{jN}} a_i a_j b_M b_N = 0$. However, a small enough perturbation of \mathbf{b} , with a corresponding perturbation of \mathbf{a} to satisfy the constraint, can be done so that $(\mathbf{b} \cdot \mathbf{m})^2$ becomes strictly positive but, by the continuity of norm and inner-product, $\|\mathbf{a}\|^2 I_4 - 2((F\mathbf{m}) \cdot \mathbf{a})^2$ stays negative.

Therefore (4.3) does not hold. Hence, we cannot say anything about the ellipticity properties of the total strain energy without further conditions on the passive strain energy. The active strain energy has a destabilising effect and there will be conditions between material parameters in the particular choice of passive strain energy (for example, stiffnesses), and the maximum active tension, that must be satisfied for ellipticity to hold. If these conditions are not met a lack of ellipticity will occur and the issues mentioned in Section 1 on singular solutions, discontinuous deformation gradients and numerical problems can occur.

However, we can derive sufficient conditions on W^{passive} for the strong ellipticity of W^{total} . Note that we can take, without loss of generality, $\|\mathbf{a}\| = \|\mathbf{b}\| = 1$ in (4.2). Now, (4.4) is minimised over unit \mathbf{a} and \mathbf{b} by taking

$$\mathbf{a} = \frac{F\mathbf{m}}{\|F\mathbf{m}\|} \quad \text{and} \quad \mathbf{b} = \mathbf{m}. \quad (4.5)$$

Note that these choices *do not* satisfy $F_{Mi}^{-1} a_i b_M = 0$, which means the following is just a sufficient condition, not a necessary one, and probably a very weak sufficient condition, as will be discussed below. Suppose we have a (physiological, say) upper bound over space and time on σ_a : let σ_{\max} be such that $\sigma_{\max} \geq \sigma_a$ for all \mathbf{X} and at every timestep. Then, using this choice of \mathbf{a} and \mathbf{b} , we have

$$\frac{\partial^2 W^{\text{active}}}{\partial F_{iM} \partial F_{jN}} a_i a_j b_M b_N \geq -\frac{\sigma_{\max}}{I_4}. \quad (4.6)$$

A sufficient condition on the passive strain energy for strong ellipticity of W^{total} is therefore

$$\frac{\partial^2 W^{\text{passive}}}{\partial F_{iM} \partial F_{jN}} a_i a_j b_M b_N > \frac{\sigma_{\max}}{I_4} \quad \forall \mathbf{a}, \mathbf{b} : \|\mathbf{a}\| = \|\mathbf{b}\| = 1, F_{Mi}^{-1} a_i b_M = 0. \quad (4.7)$$

Note that the right-hand side of this condition depends on the deformation gradient F (through I_4), and can be made unboundedly large by choosing F such that $I_4 \rightarrow 0$. In other words, the total strain energy can never be strongly elliptic for all deformation gradients, and a loss of ellipticity will occur when the fibre compression becomes too great. However, if we choose a physiological lower bound on the fibre stretch, λ_{\min} say, we can say that W^{total} will be strongly elliptic for all corresponding physiological deformation gradients if

$$\frac{\partial^2 W^{\text{passive}}}{\partial F_{iM} \partial F_{jN}} a_i a_j b_M b_N > \frac{\sigma_{\max}}{\lambda_{\min}^2} \quad \forall \mathbf{a}, \mathbf{b} : \|\mathbf{a}\| = \|\mathbf{b}\| = 1. \quad (4.8)$$

Example and discussion

Let us consider a simple isotropic strain energy. The Neo-Hookean strain energy is $W^{\text{passive}} = c_1(I_1 - 3)$ (where $I_1 = \text{tr}(C)$). Then

$$\frac{\partial^2 W^{\text{passive}}}{\partial F_{iM} \partial F_{jN}} = 2c_1 \delta_{ij} \delta_{MN} \Rightarrow \frac{\partial^2 W^{\text{passive}}}{\partial F_{iM} \partial F_{jN}} a_i a_j b_M b_N = 2c_1 \quad \text{if } \|\mathbf{a}\| = \|\mathbf{b}\| = 1.$$

Hence, we require $2c_1 > \sigma_{\max}/\lambda_{\min}^2$ for strong ellipticity to be guaranteed. Unfortunately, since cardiac tissue is anisotropic and more complex material laws are generally used in practice, an experimentally-determined value of c_1 for cardiac tissue is very difficult to find. Numerical experiments, in which we use a Mooney-Rivlin material law with contraction model (19) and pick c_1 so that the results loosely match those using the much more advanced pole-zero material ((29), with parameters given in (30)) over 200ms (see for example the implicit solution in Fig. 6) suggest a value of $c_1 \approx 10\text{kPa}$ (to the nearest order of magnitude).

A strong bound for $\sigma_{\max}/\lambda_{\min}^2$ is obtained by taking $\sigma_{\max} = 125\text{kPa}$ (using the multi-species data presented in (20)) and $\lambda_{\min} = 0.7$, giving $\sigma_{\max}/\lambda_{\min}^2 \approx 255\text{kPa}$. A weaker bound can be obtained by using the maximum value of σ_a used in the simulation, computationally determined to be just under $\sigma_{\max} = 40\text{kPa}$, and $\lambda_{\min} = 0.85$ (see Fig. 6), giving $\sigma_{\max}/\lambda_{\min}^2 \approx 55\text{kPa}$. In either case, the condition of strong ellipticity is not satisfied. This could be due to the condition being too weak—the lower bound (4.6) is probably far too weak due to the choices of \mathbf{a} and \mathbf{b} in (4.5) not satisfying the constraint $F_{Mi}^{-1} a_i b_M = 0$. An improved bound is difficult to find, and may require further assumptions on F . We leave for future work the task of improving this bound (in particular, determining an infimum and therefore obtaining a precise condition for strong ellipticity to hold or not), and the application of this to more complex passive strain energy functions.

5. The stretch-dependent but stretch-rate-independent case: $\sigma_a \equiv \sigma_a([\text{Ca}^{2+}], \lambda)$

5.1 Conditions for ellipticity

In this case, we begin with the question of classification. We now have σ_a as an function of λ . Usually this function will be unknown, even for a specific contraction model, as it will depend on the time-history of $[\text{Ca}^{2+}]$, V and \mathbf{w} . The ellipticity condition now depends on the unknown functions $\sigma_a(\lambda)$ and $\frac{\partial \sigma_a}{\partial \lambda}(\lambda)$.

The active stress once again corresponds to an active strain energy, and the strain energy can be determined, as a function of a general active tension σ_a : rewriting σ_a directly as a function of I_4 (not λ), the active tension is

$$T^{\text{active}} = \frac{\sigma_a(I_4)}{I_4} \mathbf{m} \mathbf{m}^T = \frac{\sigma_a(I_4)}{I_4} \frac{dI_4}{dC} \Rightarrow W^{\text{active}}(I_4) = \frac{1}{2} \int^{I_4} \frac{\sigma_a(I'_4)}{I'_4} dI'_4.$$

(For completeness, we note that, regarding W^{active} as a function of λ , this is equivalent to $W^{\text{active}}(\lambda) = \int^\lambda \frac{\sigma_a(\lambda')}{\lambda'} d\lambda'$).

The existence of a strain energy is not required for strong ellipticity (although without it (4.2) has to be recast as a derivative of stress rather than a second-derivative of strain energy), but it shows that we are still dealing with hyperelasticity, and in principle allows questions on the convexity or quasi-convexity or poly-convexity (31) of the strain energy,

and therefore questions on the existence of solutions, to be addressed. For strong ellipticity, it is straightforward to show that, for this case $\sigma \equiv \sigma(I_4)$, we obtain

$$\frac{\partial^2 W^{\text{active}}}{\partial F_{iM} \partial F_{jN}} a_i a_j b_M b_N = \frac{\sigma_a (\mathbf{b} \cdot \mathbf{m})^2}{I_4^2} \left(\|\mathbf{a}\|^2 I_4 - 2 ((F\mathbf{m}) \cdot \mathbf{a})^2 \right) + \frac{\sigma'_a(I_4)}{I_4} ((F\mathbf{m}) \cdot \mathbf{a})^2 (\mathbf{b} \cdot \mathbf{m})^2.$$

We derive sufficient conditions for strong ellipticity by (weakly) bounding this as in Section 4. Taking again $\|\mathbf{a}\| = \|\mathbf{b}\| = 1$, the first term is most negative when $\mathbf{a} = \frac{F\mathbf{m}}{\|F\mathbf{m}\|}$ and $\mathbf{b} = \mathbf{m}$ as before. The second term is only negative if $\sigma'_a(I_4) < 0$, in which case it is also most negative with the same choice of \mathbf{a} and \mathbf{b} . Overall, the condition (4.8) on the passive strain energy for strong ellipticity (for physiological deformation gradients) of the total energy becomes

$$\frac{\partial^2 W^{\text{passive}}}{\partial F_{iM} \partial F_{jN}} a_i a_j b_M b_N > \frac{\sigma_{\max}}{\lambda_{\min}^2} - S_{\min}, \quad \forall \mathbf{a}, \mathbf{b} : \|\mathbf{a}\| = \|\mathbf{b}\| = 1,$$

where S_{\min} is a lower bound on $\sigma'_a(I_4)$ (and could be negative), and, for any particular contraction model, is likely to have to be estimated computationally.

5.2 Choice of numerical method

This case is by far the most interesting case when considering the choice of numerical algorithm. Whereas, as explained in Section 4, the only sensible choice for the stretch- and stretch-rate-independent case is the explicit scheme; and, as will be explained in Section 6.1, the explicit scheme cannot be used in the stretch-rate-dependent case, it is not immediately clear which is the best choice of method for the stretch-only case.

The explicit method will be more computationally efficient (if the same timesteps are used for both explicit and implicit), and the question is whether the explicit algorithm is as accurate and as stable as the implicit scheme. The explicit algorithm corresponds to evaluating the stress as

$$T = 2 \frac{\partial W}{\partial C} (C^{n+1}) - p(C^{n+1})^{-1} + \frac{\sigma_a(\lambda^n)}{(\lambda^{n+1})^2} \mathbf{m} \mathbf{m}^T. \quad (5.1)$$

To study this we first consider a simplified problem analytically, before numerically investigating the explicit scheme on the full nonlinear elasticity problem.

5.2.1 The explicit method on a simplified linear problem

The explicit scheme in the stretch-dependent case (5.1) is akin to solving the simple, two-dimensional, single-unknown, quasi-static problem

$$(1 + \alpha(t, \mathbf{x})) u_{xx} + u_{yy} = 0 \quad (5.2)$$

by using the time ‘discretisation’

$$u_{xx}^{n+1} + u_{yy}^{n+1} = -\alpha(t_n, \mathbf{x}) u_{xx}^n, \quad (5.3)$$

rather than

$$(1 + \alpha(t_{n+1}, \mathbf{x})) u_{xx}^{n+1} + u_{yy}^{n+1} = 0$$

which corresponds to the implicit scheme. Here $\alpha(t, \mathbf{x})$ is analogous to the spatial derivative of the active tension $\frac{\partial \sigma_a(\lambda, t)}{\partial \lambda}$. Equation (5.3) is an extremely unusual looking semi-discretisation (and would certainly never be used as a viable method on this simple Laplace's problem), but we can gain a great deal of insight into the likely behaviour of the explicit method on the full problem by studying it.

Firstly, it should be noted that it cannot be the case that, for all α , the scheme will converge to the true solution as $\Delta t \rightarrow 0$. In particular, if α is constant and $\alpha < -1$ the PDE in the original problem (5.2) is hyperbolic, whereas the numerical scheme (5.3) involves solving a sequence of elliptic PDEs, and a hyperbolic problem can certainly not be solved by solving a sequence of elliptic problems (for one, they require different boundary conditions).

However, for $\alpha > -1$, and in particular for $|\alpha(t, \mathbf{x})| \ll 1$ for all t, \mathbf{x} , we may hope that the scheme is convergent, at $t = T$ say, as $\Delta t \rightarrow 0$ (or at worst, that the error in the $\Delta t \rightarrow 0$ limit (if it exists) is $\mathcal{O}(\alpha)$). This is not at all clear, since the method carries information from all times $t < T$ to the numerical approximation of $u(T)$. Preliminary analytic results on the $\alpha \equiv \alpha(t)$ case suggest that if the temporal refinement is such that the time is refined about some time of interest T , then if $|\alpha(t)| < 1$, and α is continuous and under certain other conditions, the scheme is indeed convergent (the proof is technical in nature and not suitable for this work). However, convergence when standard, uniform, temporal refinement is used has not been established. Such results would set computational results using the explicit scheme on the full problem on much firmer ground.

Next, note that at the first timestep, either the implicit method must be used or an artificial initial condition for u must be given. Consider an even simpler, one-dimensional, problem where $\alpha = \text{constant}$:

$$(1 + \alpha)u_{xx} = 0, \quad \text{solved with} \quad u_{xx}^{n+1} = -\alpha u_{xx}^n,$$

with boundary conditions $u = 0$ at the end-points, at all times. The solution is trivially $u(x, t) = 0$. The choice of u^0 determines the accuracy of the solution of the numerical scheme: if u^0 is correctly given as zero, $u^n = 0$ for all n . However, stability is also an issue: a small error in u will be damped away if and only if $|\alpha| < 1$, since if $u^k(x) = \epsilon(x)$ for some k and small ϵ satisfying the boundary conditions, then clearly $u^{k+n} = (-\alpha)^n \epsilon$. If $|\alpha| > 1$ then $\|u^n\| \rightarrow \infty$ as $n \rightarrow \infty$. We have, in this case, *conditional stability* (conditional on α).

Equations (5.2) and (5.3) are also amenable to stability analysis, assuming a spatial discretisation is chosen, and serves to illustrate another important point. Let u^0 and \tilde{u}^0 be two nearby initial conditions, and let $v^n = u^n - \tilde{u}^n$. The scheme is stable if v^n does not get amplified as n increases. v^n satisfies

$$v_{xx}^{n+1} + v_{yy}^{n+1} = -\alpha(t_n, \mathbf{x})v_{xx}^n.$$

The spatial-discretised counterpart of this equation is

$$A\mathbf{v}^{n+1} = -B_n\mathbf{v}^n,$$

where v_i^{n+1} is the value of $v^n(x)$ at the i -th node, and A and B_n are matrices corresponding to the discretisations of the $\frac{\partial^2}{\partial x^2} + \frac{\partial^2}{\partial y^2}$ and $\alpha(t_n, \mathbf{x})\frac{\partial^2}{\partial x^2}$ operators, respectively. Since $\mathbf{v}^{n+1} = -A^{-1}B_n\mathbf{v}^n$, stability is determined based on the eigenvalues of the matrices $A^{-1}B_n$.

First, consider the case $\alpha = \text{constant}$. Then $B_n = \alpha B^*$ for some B^* , and the update matrix is $-\alpha A^{-1} B^*$. If all the eigenvalues of this matrix have moduli less than one (or equal to one if the corresponding eigenspace is one-dimensional), the scheme is stable; otherwise the scheme is unstable. It is clear that the scheme will be stable for small enough α (i.e. $0 \leq |\alpha| < 1/\rho(A^{-1} B^*)$, where $\rho(A^{-1} B^*)$ is the spectral radius of $A^{-1} B^*$); and unstable for large enough α ($|\alpha| > 1/\rho(A^{-1} B^*)$)—i.e. again, conditional stability. It is important to note that the stability criterion is a condition on α and perhaps the spatial stepsize Δx (implicitly contained in A and B^*), and *not on the timestep* Δt . Δt has a bearing on the accuracy of the scheme but not its stability, essentially since there are no time-derivatives being discretised. This is in contrast to, for example, the classical problem of Euler's method on the diffusion equation, where the error is dependent on Δt (and Δx) and the stability criterion is that the Courant number $\Delta t/\Delta x^2$ must be less than $1/4$. Unlike the diffusion equation, with (5.3) an unstable solution cannot be made stable by decreasing Δt .

In the spatially-independent α case, $\alpha \equiv \alpha(t)$ only, then $B_n = \alpha(t_n) B^*$. Although the update matrix now varies each timestep, the eigenvectors are constant and the eigenvalues are just the eigenvalues of $A^{-1} B^*$ scaled by $\alpha(t_n)$, so it is easy to see that if $\alpha(t)$ is bounded below $1/\rho(A^{-1} B^*)$, then small errors be damped away, so that the scheme is stable. If, say, there exists T such that $\alpha(t)$ is bounded above $1/\rho(A^{-1} B^*)$ for all $t > T$, then errors can be magnified and the scheme will be unstable. In the $\alpha \equiv \alpha(t, \mathbf{x})$ case such characterisations are not so simple to state, but we would expect stability if $\|\alpha(t, \cdot)\|$ is small enough, again independently of the timestep. This is the behaviour we now search for in the full nonlinear problem.

5.2.2 The explicit method on the nonlinear elasticity problem

The explicit scheme on the full elasticity problem, (5.1), is too complex for a similar stability analysis, so instead we numerically search for the similar behaviour. We use three choices of σ_a : The first two are simple, non-physiological, contraction models, chosen so that behaviour exhibited by the explicit scheme on these very simple models can be attributed to the scheme itself, and not, say, on nonlinearities in σ_a or on solving ODEs. These two contraction models are

$$\begin{aligned}\sigma_a^{(1)}(t) &= k|\sin t| \\ \sigma_a^{(2)}(t, \lambda) &= k\lambda|\sin t|\end{aligned}$$

and here we take the passive material response to be Neo-Hookean with stiffness c_1 . The third contraction model, $\sigma_a^{(3)}$, is the model described in (19), a relatively simple contraction model containing a single ODE in the length of myocyte contractile unit. For this we use the pole-zero passive strain energy (29), with parameters given in (30).

The simulations we run are two-dimensional simulations on the unit square (1cm by 1cm), with fibres in the X -direction, and with the $X = 0$ side fixed in space (and electrically stimulated for the $\sigma_a^{(3)}$ case). Plotted is the x -position of the bottom-right corner of the square, i.e. $x(1, 0)$, and is therefore a measure of the contraction in the fibre-direction (and an approximation of λ at that point).

Now, since the contraction model $\sigma_a^{(1)}$ is independent of stretch, we expect the explicit and implicit schemes to give exactly identical results for this contraction model, and this is

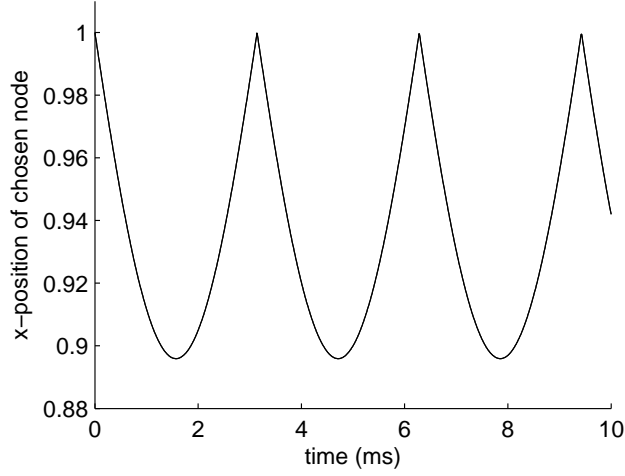


Fig. 3 The results of the explicit and implicit schemes using the stretch-independent contraction model $\sigma_a^{(1)}$. Both schemes give exactly identical results.

indeed the case. The solutions of both methods on this model are given in Fig. 3. Here we have taken $k = c_1$ (note: using the results in Section 4, strong ellipticity then is guaranteed to hold if $\lambda_{\min} > 2^{-1/2} \approx 0.707$, which appears to be the case given the results).

Fig. 4 displays the results of the use of the stretch-dependent contraction model $\sigma_a^{(2)}$, with $k = c_1$. Using the results in Section 5.1, and the fact the $\frac{d\sigma_a^{(2)}}{d\lambda} \geq 0$, strong ellipticity then is again guaranteed to hold if $\lambda_{\min} > 2^{-1/2}$. Both methods turn out to be stable with this choice of k so we can use this figure to study the error introduced by using the explicit scheme over the implicit approach. Fig. 4(a)-(c) give the results for both schemes using timesteps $\Delta t = 0.01, 0.1$ and 1 respectively. Since the implicit solution at any time does not depend on the solution at any previous time, the implicit solution should take the same values regardless of Δt (as does the true solution), and this is observed (see Fig. 4(c)). The explicit scheme we hope converges to the solution of the implicit scheme as $\Delta t \rightarrow 0$, and this appears to be the case. In fact, there is very little difference between the schemes for small Δt ($\Delta t = 0.01$ and 0.1), but there is some error (although not large error) in the explicit scheme for $\Delta t = 1$.

However, now consider the case $k = 5c_1$, for which results are given in Fig. 5. With $\Delta t = 0.01$, the implicit method has no problems but the explicit scheme fails (Fig. 5(a)—results are plotted until failure), through the Newton method failing to converge (specifically, computing a direction in which the residual does not decrease). We attribute this failure to instability[†]. Decreasing the timestep does not remove the instability, as shown in Fig. 5(b),

[†] Attributing this failure to instability is not as simple as it could have been, complicated by the fact that strong ellipticity is not guaranteed for this choice of k . However, there are a few reasons why it could be argued that it is instability that causes the failure, rather than a loss of strong ellipticity. Firstly, the criteria derived in Section 5.1 were only sufficient conditions for ellipticity, not necessary, so it is not clear if ellipticity has been lost for this choice of k . Also, the implicit scheme does not fail, suggesting the issue

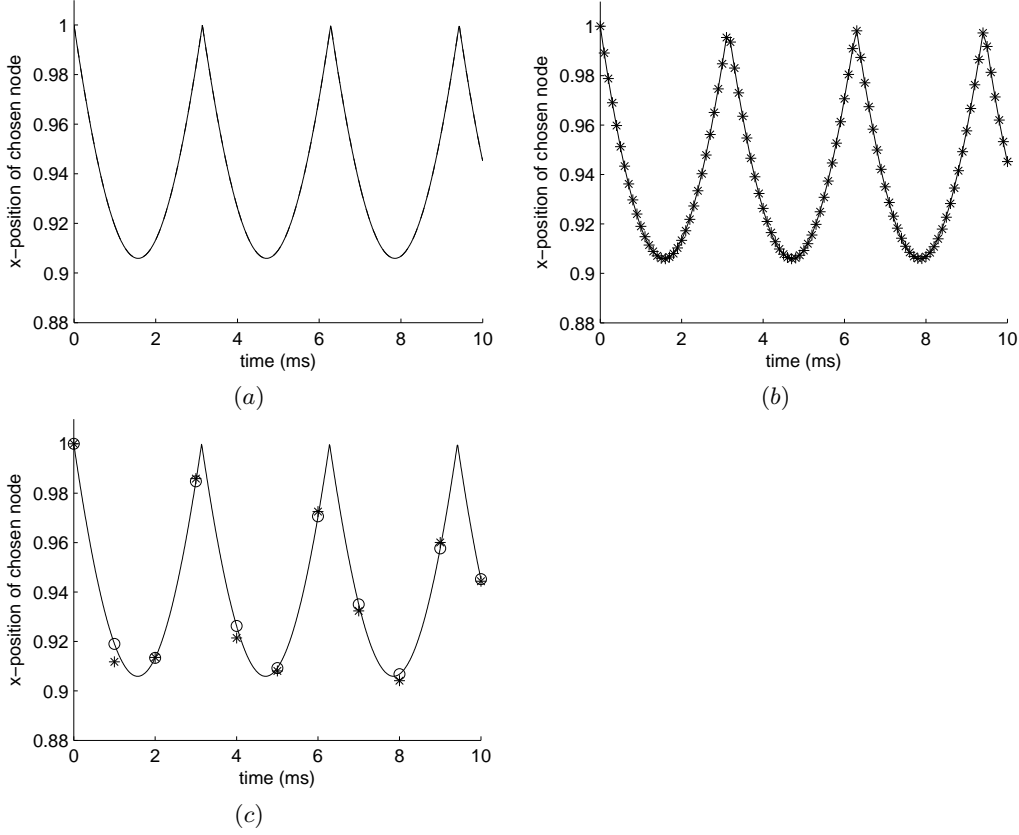


Fig. 4 Comparison of *error* in the explicit and implicit schemes in the *stable case* ($\sigma_a^{(2)}$ with $k = c_1$). (a) $\Delta t = 0.01$, explicit (solid line) and implicit (dashed line) results are visually indistinguishable. (b) $\Delta t = 0.1$, explicit (stars) and implicit (solid line) are still essentially indistinguishable. (c) Implicit with $\Delta t = 1$ (circles) coincident with implicit with $\Delta t = 0.01$ (solid line); but explicit with $\Delta t = 1$ is noticeably different.

which is expected from the analysis of (5.3). However, increasing the spacestep Δx from 0.2 to 1 does allow the explicit scheme to run without failure, although at an obvious loss of accuracy. Note that we are not saying that in general *increasing* the spacestep may remove instabilities, just that *changing* it might—it is not clear how the stability criterion for (5.1) will depend on Δx .

Finally, Fig. 6 plots the results of the two schemes with the physiological contraction model $\sigma_a^{(3)}$, over 100ms. Again, the implicit scheme has no problems, but the explicit scheme, with $\Delta x = 0.1\text{cm}$ and $\Delta t = 0.01\text{ms}$, fails after 7.6ms. It has been verified that the explicit scheme also fails when $\Delta t = 0.001\text{ms}$, after about 6.7ms. For this contraction

is with the method not the problem. Finally, the characteristics of these failures with varying Δt and Δx match those expected for instabilities.

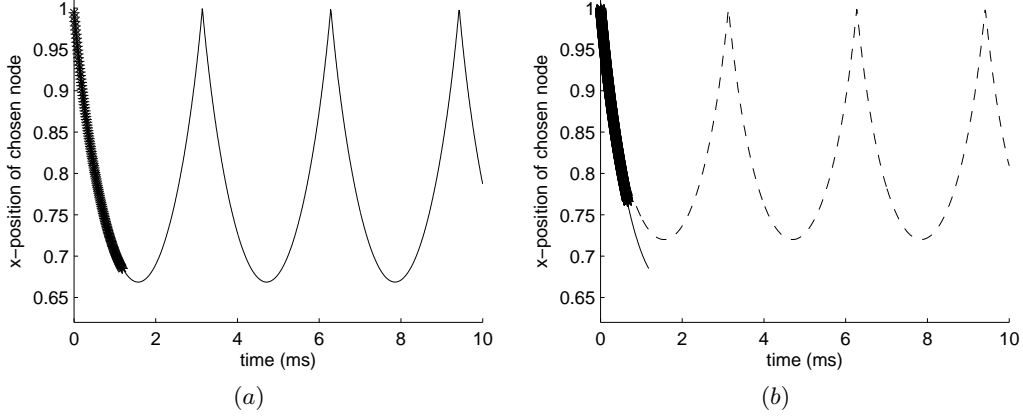


Fig. 5 The *unstable case* ($\sigma_a^{(2)}$ with $k = 5c_1$). (a) The implicit scheme (solid line) is stable but the explicit scheme (stars) fails ($\Delta t = 0.01$ for both). (b) All explicit: decreasing Δt does not fix the instability but changing Δx does. Explicit with $\Delta x = 0.2$, $\Delta t = 0.01$ (thin solid line); explicit with $\Delta x = 0.2$, $\Delta t = 0.0001$ (stars, i.e. thick line); explicit with $\Delta x = 1$, $\Delta t = 0.01$ (dashed line).

model, increasing Δx to 1cm fails to fix the instability, as also shown in the figure. There may be values of Δx for which the explicit scheme is stable for this contraction model, but they may lead to large errors if greater than 1cm, and the implicit scheme is clearly far superior. Note again that, even without the stability issues, the implicit scheme can be superior: a greater timestep can be used for the implicit scheme making it potentially more computationally efficient.

6. The stretch- and stretch-rate-dependent case: $\sigma_a \equiv \sigma_a([\text{Ca}^{2+}], \lambda, \dot{\lambda})$

We begin by explaining why the explicit method cannot be used when stretch-rate-dependent contraction models are employed.

6.1 The failure of the explicit method on stretch-rate-dependent problems

For clarity, we make use of an analogous 1D problem to illustrate the bad time-discretisation at the heart of the explicit method on stretch-rate-dependent problems. Consider an ‘active’ 1D linearly-elastic rod. The stress, σ , satisfies

$$\frac{\partial \sigma}{\partial x} = 0.$$

Letting the strain be denoted $\epsilon = \partial u / \partial x$, the linear nature of the rod means the passive part of the stress is linear in the strain, i.e. $\sigma^{\text{passive}} = c_1 \epsilon$. Suppose the active stress is linear in the difference between the strain and some preferred strain $\alpha(t)$ (corresponding to the dependence of σ_a on λ and the electrophysiology), and linear in the strain rate (corresponding to the dependence of σ_a on $\dot{\lambda}$), so that $\sigma^{\text{active}} = c_2(\epsilon - \alpha(t)) + c_3 \dot{\epsilon}$. Therefore

$$\frac{\partial}{\partial x} \left(c_1 \frac{\partial u}{\partial x} + c_2 \left(\frac{\partial u}{\partial x} - \alpha(t) \right) + c_3 \frac{\partial^2 u}{\partial x \partial t} \right) = 0, \quad (6.1)$$

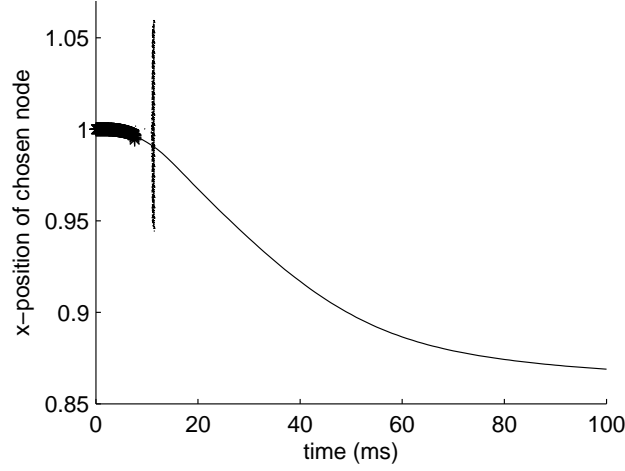


Fig. 6 Simulations with the physiological, stretch-dependent, contraction model $\sigma_a^{(3)}(\lambda)$ from (19). The implicit scheme (solid line) has no problems but the explicit scheme with either $\Delta t = 0.01\text{ms}$, $\Delta x = 0.1\text{cm}$ (stars, i.e. thick line), or $\Delta t = 0.01\text{ms}$, $\Delta x = 1\text{cm}$ (dotted line) both fail.

with appropriate initial and boundary conditions. Now, consider three time-discretisations of (6.1):

$$\begin{aligned} c_1 u_{xx}^{m+1} + c_2 (u_{xx}^{m+1} - \alpha(t^{m+1})) + c_3 \frac{u_{xx}^{m+1} - u_{xx}^m}{\Delta t} &= 0, \\ c_1 u_{xx}^m + c_2 (u_{xx}^m - \alpha(t^{m+1})) + c_3 \frac{u_{xx}^{m+1} - u_{xx}^m}{\Delta t} &= 0, \\ c_1 u_{xx}^{m+1} + c_2 (u_{xx}^m - \alpha(t^{m+1})) + c_3 \frac{u_{xx}^m - u_{xx}^{m-1}}{\Delta t} &= 0. \end{aligned}$$

The first discretisation is a fully implicit discretisation and corresponds to the ‘implicit algorithm’ for solving cardiac mechanics. The second discretisation is a classical explicit discretisation. This discretisation has, as far as we are aware, not been used in cardiac electromechanical problems. It may lead to stability conditions on timestep and spacestep. The third discretisation corresponds to the ‘explicit algorithm’ as described in this paper, but contains the following time-discretisation:

$$\dot{y} = f(t, y) \quad \text{solved by} \quad f(t^{n+1}, y^{n+1}) = \frac{y^n - y^{n-1}}{\Delta t}.$$

This is clearly a bad discretisation, as shown by trying it on[†] $\dot{y} = y$, $y(0) = 1$. This explains why the explicit algorithm fails with stretch-rate-dependent contraction models. Fig. 7

[†] Suppose $\dot{y} = f(t, y)$ is solved using: y^0, y^1 given, $f(t^{n+1}, y^{n+1}) = \frac{y^n - y^{n-1}}{\Delta t}$. Firstly, for simple ODEs such that $f \equiv f(t)$ only, this makes no sense—we would have to assume y^1 is not given, and then we obtain Euler’s method. Consider the simplest ODE such the f is dependent on y , $f(t, y) = ky$. For any k and any Δt we have: $y^0 = 1$, $y^1 = e^{k\Delta t}$ (exact solutions) $\Rightarrow y^2 = k + \mathcal{O}(\Delta t)$, $y^3 = \frac{k-1}{\Delta t} + \mathcal{O}(1)$, illustrating that the scheme is not convergent nor stable.

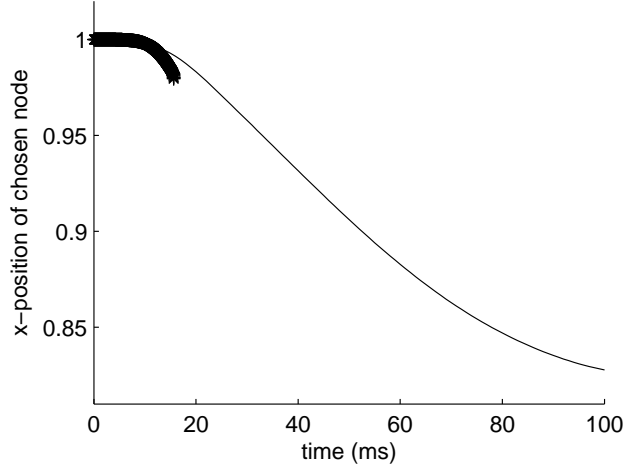


Fig. 7 The implicit scheme (solid line) on the stretch- and stretch-rate-dependent contraction model described in (20), and the failure of the explicit scheme (stars, i.e. thick line) with the same model.

illustrates the failure of the explicit method on the stretch-rate dependent NHS contraction model (20), again through the Newton solver failing to converge, after about 15ms. The implicit method, in contrast, has no problems (as was shown in (5)).

It is worth verifying, for a particular contraction model, that σ_a really is a function of $\dot{\lambda}$ —in principle, since the contraction models are ODE-based, the dependence on the time-derivative of λ could be integrated away when solving the ODEs. We look at the NHS model. Here, σ_a is an algebraic function of three particular state variables Q_i ($i = 1, 2, 3$), and Q_i is a function of the time history of $\dot{\lambda}$ as fading-memory model

$$Q_i = A_i \int_{-\infty}^t e^{-\alpha_i(t-\tau)} \dot{\lambda}(\tau) d\tau,$$

where A_i and α_i are parameters. If $\alpha_i = 0$ (or small), then $Q_i = A_i(\lambda - 1)$, but otherwise there is a contribution from $\dot{\lambda}(t)$ (while the remainder of time-history of $\dot{\lambda}$, i.e. $\{\dot{\lambda}(\tau), \tau < t\}$, can be considered to be known). We need any α_i to be not small for σ_a to be a function of $\dot{\lambda}$. Their values are 30s^{-1} , 130s^{-1} , 635s^{-1} respectively, so the largest is 0.625ms^{-1} , which is not small enough to approximate Q_i with $A_i\lambda$.

6.2 Mathematical analysis of the canonical problem

For the cases where the contraction model was independent of stretch-rate, analysis of the mathematical formulation was tractable without the need to consider simplifications of the governing equations: we were able to show hyperelasticity still holds and consider classification (strong ellipticity) whilst staying in the framework of nonlinear elasticity with general material laws and fibre directions. When investigating the numerics however, and in particular the explicit scheme in the stretch-dependent case, we chose to study a simpler problem which was more analytically tractable.

For contraction models which depend on the stretch-rate, a mathematical analysis of the governing equations appears more difficult, and for this paper we simplify the problem in order to gain insight. As initial simplifying assumptions, let us assume isotropic linear elasticity, and take the fibres to be everywhere parallel to the X -axis. Writing $\mathbf{u} = \mathbf{x} - \mathbf{X}$ for the displacement, and $\mathbf{x} = (x, y, z)$, $\mathbf{u} = (u, v, w)$ etc, the linearised fibre stretch is then given by $\lambda = \frac{\partial x}{\partial X} = \frac{\partial u}{\partial X} - 1$, so the fibre stretch-rate is $\dot{\lambda} = \frac{\partial^2 u}{\partial X \partial t}$.

As before

$$\sigma = \sigma^{\text{passive}} + \sigma^{\text{active}},$$

where now, due to the assumption of isotropic linear elasticity, $\sigma_{ij}^{\text{passive}} = 2\mu_L \epsilon_{ij} + \lambda_L \epsilon_{kk} \delta_{ij}$ (where μ_L and λ_L are the standard linear elasticity Lamé coefficients), and, to leading order

$$\sigma_{ij}^{\text{active}} = \sigma_a(u_X - 1, u_{Xt}) \delta_{1i} \delta_{1j},$$

where the active tension is σ_a some nonlinear function of λ and $\dot{\lambda}$. The divergence of the active stress then satisfies

$$\begin{aligned} \frac{\partial \sigma_{ij}^{\text{active}}}{\partial X_j} &= \frac{\partial}{\partial X} (\sigma_a(u_X - 1, u_{Xt}) \delta_{1i}), \\ &= \left(\frac{\partial \sigma_a}{\partial u_X} u_{XX} + \frac{\partial \sigma_a}{\partial u_{Xt}} u_{XXt} \right) \delta_{1i}, \end{aligned}$$

so, the equilibrium equation (assuming zero body force) $\frac{\partial \sigma_{ij}}{\partial X_j} = 0$ gives us the three equations:

$$\begin{aligned} \frac{\partial \sigma_{1j}^{\text{passive}}}{\partial X_j} + \left(\frac{\partial \sigma_a}{\partial u_X} u_{XX} + \frac{\partial \sigma_a}{\partial u_{Xt}} u_{XXt} \right) &= 0, \\ \frac{\partial \sigma_{2j}^{\text{passive}}}{\partial X_j} &= 0, \\ \frac{\partial \sigma_{3j}^{\text{passive}}}{\partial X_j} &= 0. \end{aligned}$$

Overall, we have one third-order, time-dependent equation, coupled to two static, standard elasticity, equations.

Here, we just consider the first of these equations, uncoupling it from the latter two equations, and simplify it further to a single ‘canonical’ PDE in one unknown, u , over 2D space (and now writing the independent variable as \mathbf{x} not \mathbf{X}):

$$u_{xxt} = -(u_{xx} + u_{yy}), \quad (6.2)$$

The negative choice of sign is just so solutions will tend to decay with time as would be expected. The questions that can be asked for this problem are: of what type is it, what are appropriate boundary and initial conditions, do solutions exist and are they unique, and what is an accurate numerical scheme for it?

In this paper we make a couple of observations on this equation; a detailed analysis of (6.2), let alone of the full nonlinear elasticity problem, is left for future work. Firstly,

it can be noted that (6.2) is reminiscent of the equations of visco-elasticity, although there are some important differences. Consider a simple linear Voigt visco-elastic model, where the stress σ is related to the strain e by (32) $\sigma = Ee + \eta\dot{e}$, where E is the elastic stiffness and η the viscosity. The corresponding canonical PDE to (6.2) for Voigt visco-elasticity is therefore

$$u_{xxt} + u_{yyt} = -(u_{xx} + u_{yy}). \quad (6.3)$$

A significant difference between these two canonical forms can be seen when considering characteristic surfaces for each. Characteristic surfaces are surfaces \mathcal{S} in space-time for which the prescription of lower-order derivatives of u on \mathcal{S} does not then uniquely determine the highest-order derivatives of u (33). The Cauchy-Kowalewski theorem (33) states that the Cauchy problem—determining a local solution of the PDE given prescribed smooth, compatible data (u and lower-order derivatives of u) on a surface \mathcal{S}_0 —has a solution if \mathcal{S}_0 is not a characteristic surface. Let us write a characteristic surface \mathcal{S} as $\phi(t, x, y) = \text{const}$, with normal (ϕ_t, ϕ_x, ϕ_y) . The characteristic surfaces for (6.2), the canonical problem corresponding to cardiac electromechanics, are given by (33)

$$\phi_t \phi_x^2 = 0, \quad (6.4)$$

whereas the characteristic surfaces for (6.3), the canonical problem corresponding to visco-elasticity, are given by

$$\phi_t(\phi_x^2 + \phi_y^2) = 0.$$

Both equations have a solution $\phi_t = 0$, corresponding to characteristic surfaces which are orthogonal to the (x, y) -plane (the (x, y) -plane being the surface initial conditions will usually be prescribed on). The visco-elastic case also has a solution $\phi_x = \phi_y = 0$, corresponding to surfaces $t = \text{const}$. For (6.4) however, there is a larger family of characteristic surfaces given by $\phi_x = 0$, which corresponds to surfaces which, for a given t , lie entirely along a single fibre (i.e parallel to the fibre direction). Thus the Cauchy problem for the canonical electromechanics PDE, in contrast to the canonical visco-elasticity PDE, has no solutions if the data is prescribed on a surface parallel to a fibre at each fixed t .

In practice of course we do not want to solve the Cauchy problem; instead we would like existence and uniqueness of solutions using a standard prescription of an initial condition at $t = 0$ and a mixture of u and $\nabla u \cdot \mathbf{n}$ on the boundary. However, we now show how (6.2) can require fairly strong compatibility conditions to hold between the initial conditions and the boundary conditions for a solution to exist. Let us take the domain to be the unit square, $\Omega = [0, 1] \times [0, 1]$, and consider the pure Neumann problem, where we prescribe

$$\begin{aligned} u(0, x, y) &= u_0(x, y), \\ \nabla u \cdot \mathbf{n} &= 0 \quad \text{on } \partial\Omega, \end{aligned}$$

and assume that u_0 satisfies the boundary conditions, i.e. $\nabla u_0 \cdot \mathbf{n} = 0$. It is easy to see that the solution of the visco-elasticity PDE (6.3) is simply

$$u(t, x, y) = e^{-t}u_0(x, y) + c(t)$$

for some arbitrary function $c(t)$ with $c(0) = 0$. The uniqueness of this solution, up to the arbitrary function of t , is straightforward to show using elementary techniques. Now

consider (6.2). Since u_0 satisfies zero-Neumann boundary conditions, let us expand it as a Fourier cosine-series

$$u_0(x, y) = \sum_{n, m \geq 0} k_{mn} \cos(m\pi x) \cos(n\pi y),$$

and similarly expand the solution as

$$u(t, x, y) = \sum_{n, m \geq 0} \alpha_{mn}(t) \cos(m\pi x) \cos(n\pi y), \quad (6.5)$$

for some functions $\alpha_{mn}(t)$ to be determined. Substituting this into the PDE (6.2), we obtain the following ODE for each α_{mn} :

$$-m^2 \dot{\alpha}_{mn} = (m^2 + n^2) \alpha_{mn}, \quad \alpha_{mn}(0) = k_{mn}$$

For $m > 0$, this gives $\alpha_{mn} = e^{-(1+\frac{n^2}{m^2})t} k_{mn}$. For $m = n = 0$, we have no information about $\alpha_{00}(t)$ other than the initial condition, but this just says that, as with the visco-elastic solution, we can add any arbitrary function of t to the solution, i.e. $\alpha_{00}(t) = k_{00} + c(t)$, for any $c(t)$ with $c(0) = 0$. The case $m = 0, n > 0$ however, tells us that $\alpha_{0n}(t) \equiv 0$ if $n \geq 1$. But $\alpha_{0n}(0) = k_{0n}$, so a solution of the PDE exists *only if* $k_{0n} = 0$ for all $n \geq 1$. For example, this pure-Neumann problem has no solution if $u_0(x, y) = g(y)$ for some $g \not\equiv 0$. Thus, in contrast to the visco-elastic case, the imposition of pure Neumann boundary conditions introduces a condition on the initial condition (and not just on the boundary; throughout the domain), which must be satisfied for a solution to exist.

This example illustrates how degeneracy in the equations—the lack of any y -derivatives in the highest order derivatives—affects the existence of solutions, and that more care than usual may have to be taken when prescribing initial and boundary conditions. Note that if zero-Dirichlet boundary conditions are prescribed on the surfaces *parallel* to the fibre direction, the arbitrary function $c(t)$ is removed from the solution but the constraint on the initial condition is still present. However, if zero-Dirichlet boundary conditions are prescribed on the surfaces *perpendicular* to the fibres, the constraint on the initial condition is no longer required.

The aim of this section was simply to write down the basic canonical PDE corresponding to the PDEs of nonlinear elasticity coupled to stretch-rate-dependent contraction models, and make a few preliminary observations on it. The task of performing a full analysis of this canonical problem, determining if such observations follow through to the nonlinear elasticity setting, and if so deciding how they affect computational modelling in practice, is a significant task, and one which we leave for future work.

7. Conclusions

In this paper we have identified the fact that choosing a contraction model which is dependent on the fibre-stretch, or the fibre-stretch and stretch-rate, can have a fundamental impact on both the type of mathematical problem being solved, and on the appropriate choice of numerical scheme. We have introduced a categorisation of contraction models based on whether they: (i) depend only on cellular electrical activity, and are not dependent on the deformation; (ii) depend on the stretch in the fibre direction; or (iii) depend on both

the stretch and stretch-rate in the fibre direction. For each category, we have investigated the type of PDE which arises, and studied the accuracy of the explicit and implicit numerical methods. In this paper, we have restricted ourselves to such weakly coupled models only. However, the analysis still formally holds for strongly-coupled electro-mechanics systems in which the cell model and contraction model are replaced with a single ODE system, as long as that ODE system is dependent on the deformation through the stretch and stretch-rate, and provides an active tension that contributes additively to the bulk stress. This is because the manner in which the active tension depends on the electro-physiology, whether it is through the calcium transient, or the voltage, or in a more tightly-coupled manner, has no effect on the analysis. However, the implicit algorithm without alterations may become computationally untractable for such models: re-integrating a contraction model (generally small systems of ODEs) every time a stress is evaluated is not overly computationally demanding, whereas re-integrating a model that also contains a cell-model (generally very large systems of ODEs) every time a stress is evaluated would be significantly more expensive.

In terms of numerical solution schemes, we have described how the explicit method is the only sensible choice for contraction models which do not depend on the stretch or stretch-rate; but how in the stretch and stretch-rate-dependent case the explicit method involves using an unjustifiable time-discretisation. In the middle case, when the contraction model just depends on the stretch, both schemes are viable (in particular, the explicit scheme may be convergent (i.e. accurate)), but it is conditionally unstable, with the stability criterion depending on the contraction model and (perhaps) the spatial stepsize, but not the timestep.

For contraction models which do not depend on stretch-rate, we have shown the existence of a total strain energy function (which includes the active response of the tissue), and discussed under what conditions this total strain energy is strongly elliptic. This would allow us to preclude certain types of unnatural material behaviour. Unfortunately, however, the sufficient conditions that were derived do not appear to hold in practice. We have left it as an open problem to derive better sufficient conditions for strong elasticity, or to explicitly prove the lack of strong ellipticity for given strain energy functions and contraction models. For contraction models which are dependent on the stretch-rate, the situation is far more complicated, since the problem is a third-order PDE involving mixed derivatives. We have introduced a simple third-order ‘canonical’ PDE which was amenable to some mathematical analysis and suggested that, in this case, there may be situations where boundary conditions and initial conditions need to be considered together, with certain combinations leading to a non-existence of solutions. However, a number of questions are still very much left open, and these will be pursued in future work.

Acknowledgements

PP is supported by the EPSRC-funded OXMOS project *New frontiers in the mathematics of solids*, (grant reference EP/D048400/1). JPW is supported by Award No. KUK-C1-013-04, made by King Abdullah University of Science and Technology (KAUST). PP would also like to gratefully acknowledge the help of Steven Niederer (Oxford University Computing Laboratory) and Endre Süli (Oxford University Mathematical Institute).

References

1. L. Zee and E. Sternberg. Ordinary and strong ellipticity in the equilibrium theory of incompressible hyperelastic solids. *Archive for Rational Mechanics and Analysis* **83**(1) (1983) 53–90.
2. G. Holzapfel, T. Gasser, and R. Ogden. A new constitutive framework for arterial wall mechanics and a comparative study of material models. *Journal of elasticity* **61**(1) (2000) 1–48.
3. S. Antman. *Nonlinear Problems of Elasticity*. Springer (1995).
4. G. Holzapfel, T. Gasser, and R. Ogden. Comparison of a multi-layer structural model for arterial walls with a Fung-type model, and issues of material stability. *Journal of biomechanical engineering* **126** (2004) 264.
5. P. Pathmanathan and J. Whiteley. A numerical method for cardiac mechanoelectric simulations. *Annals of Biomedical Engineering* **37**(5) (2009) 860–873.
6. J. Whiteley, M. Bishop, and D. Gavaghan. Soft tissue modelling of cardiac fibres for use in coupled mechano–electric simulations. *Bull. Math. Biol.* **69** (2007) 2199–2225.
7. S. Niederer and N. Smith. An improved numerical method for strong coupling of excitation and contraction models in the heart. *Progress in Biophysics and Molecular Biology* **96**(1–3) (2008) 90–111.
8. J. Keener and J. Sneyd. *Mathematical physiology*, volume 8 of *Interdisciplinary applied mathematics*. Springer (1998).
9. R. Ogden. *Non-linear elastic deformations*. Dover Pubns (1997).
10. L. Xia, M. Huo, Q. Wei, F. Liu, and S. Crozier. Analysis of cardiac ventricular wall motion based on a three-dimensional electromechanical biventricular model. *Physics in Medicine and Biology* **50**(8) (2005) 1901–1917.
11. C. Cherubini, S. Filippi, P. Nardinocchi, and L. Teresi. An electromechanical model of cardiac tissue: Constitutive issues and electrophysiological effects. *Progress in Biophysics and Molecular Biology* **97**(2–3) (2008) 562–573.
12. P. Nardinocchi and L. Teresi. On the Active Response of Soft Living Tissues. *Journal of Elasticity* **88**(1) (2007) 27–39.
13. P. Kohl, F. Sachs, and M. Franz. *Cardiac mechano-electric feedback and arrhythmias: from pipette to patient*. WB Saunders Co (2005).
14. P. Kohl, C. Bollensdorff, and A. Garny. Electrophysiological Effects of Mechano-Sensitive Ion Channels on Ventricular Electrophysiology: Experimental and Theoretical Models. *Experimental Physiology* **91**.2 (2006) 307–321.
15. M. Franz, R. Cima, D. Wang, D. Profitt, and R. Kurz. Electrophysiological effects of myocardial stretch and mechanical determinants of stretch-activated arrhythmias. *Circulation* **86**(3) (1992) 968–978.
16. E. Nevo and Y. Lanir. Structural finite deformation model of the left ventricle during diastole and systole. *Journal of biomechanical engineering* **111** (1989) 342.
17. M. Nash and A. Panfilov. Electromechanical model of excitable tissue to study reentrant cardiac arrhythmias. *Progress in biophysics and molecular biology* **85**(2–3) (2004) 501–522.
18. M. Sermesant, H. Delingette, and N. Ayache. An electromechanical model of the heart for image analysis and simulation. *IEEE transactions on medical imaging* **25**(5) (2006) 612–625.

19. R. Kerckhoffs, P. Bovendeerd, F. Prinzen, K. Smits, and T. Arts. Intra-and interventricular asynchrony of electromechanics in the ventricularly paced heart. *Journal of Engineering Mathematics* **47(3)** (2003) 201–216.
20. S. Niederer, P. Hunter, and N. Smith. A quantitative analysis of cardiac myocyte relaxation: a simulation study. *Biophysical journal* **90(5)** (2006) 1697–1722.
21. H. Watanabe, S. Sugiura, H. Kafuku, and T. Hisada. Multiphysics simulation of left ventricular filling dynamics using fluid-structure interaction finite element method. *Biophysical journal* **87(3)** (2004) 2074–2085.
22. T. Usyk, R. Mazhari, and A. McCulloch. Effect of laminar orthotropic myofiber architecture on regional stress and strain in the canine left ventricle. *Journal of Elasticity* **61(1)** (2000) 143–164.
23. J. Rice, F. Wang, D. Bers, and P. de Tombe. Approximate model of cooperative activation and crossbridge cycling in cardiac muscle using ordinary differential equations. *Biophysical Journal* **95(5)** (2008) 2368–2390.
24. P. Hunter, A. McCulloch, and H. Ter Keurs. Modelling the mechanical properties of cardiac muscle. *Progress in biophysics and molecular biology* **69(2-3)** (1998) 289–331.
25. N. Smith, M. Buist, and A. Pullan. Altered T wave dynamics in a contracting cardiac model. *Journal of cardiovascular electrophysiology* **14(s10)** (2003) 203–209.
26. J. Reddy. *An Introduction to the Finite Element Method*. McGraw–Hill (1993).
27. P. Pathmanathan. *Predicting Tumour Location by Simulating the Deformation of the Breast using Nonlinear Elasticity and the Finite Element Method*. D.Phil thesis, University of Oxford (2007).
28. J. Walton and J. Wilber. Sufficient conditions for strong ellipticity for a class of anisotropic materials. *International Journal of Non-Linear Mechanics* **38(4)** (2003) 441–455.
29. M. Nash and P. Hunter. Computational mechanics of the heart. *Journal of elasticity* **61(1)** (2000) 113–141.
30. E. Remme, M. Nash, and P. Hunter. Distributions of myocyte stretch, stress and work in models of normal and infarcted ventricles. *Cardiac Mechano-Electric Feedback and Arrhythmias*, pages 381–391 (2005).
31. J. Ball. Convexity conditions and existence theorems in nonlinear elasticity. *Archive for rational mechanics and Analysis* **63(4)** (1976) 337–403.
32. P. Howell, G. Kozyreff, and J. Ockendon. *Applied Solid Mechanics*. Cambridge University Press (2008).
33. F. John. *Partial differential equations*. Springer (1991).

List of Figures

1	Components of cardiac electromechanical models.	4
2	Schematic of the implicit algorithm.	9
3	The results of the explicit and implicit schemes using the stretch-independent contraction model $\sigma_a^{(1)}$. Both schemes give exactly identical results.	16
4	Comparison of <i>error</i> in the explicit and implicit schemes in the <i>stable case</i> ($\sigma_a^{(2)}$ with $k = c_1$). (a) $\Delta t = 0.01$, explicit (solid line) and implicit (dashed line) results are visually indistinguishable. (b) $\Delta t = 0.1$, explicit (stars) and implicit (solid line) are still essentially indistinguishable. (c) Implicit with $\Delta t = 1$ (circles) coincident with implicit with $\Delta t = 0.01$ (solid line); but explicit with $\Delta t = 1$ is noticeably different.	17
5	The <i>unstable case</i> ($\sigma_a^{(2)}$ with $k = 5c_1$). (a) The implicit scheme (solid line) is stable but the explicit scheme (stars) fails ($\Delta t = 0.01$ for both). (b) All explicit: decreasing Δt does not fix the instability but changing Δx does. Explicit with $\Delta x = 0.2$, $\Delta t = 0.01$ (thin solid line); explicit with $\Delta x = 0.2$, $\Delta t = 0.0001$ (stars, i.e. thick line); explicit with $\Delta x = 1$, $\Delta t = 0.01$ (dashed line).	18
6	Simulations with the physiological, stretch-dependent, contraction model $\sigma_a^{(3)}(\lambda)$ from (19). The implicit scheme (solid line) has no problems but the explicit scheme with either $\Delta t = 0.01\text{ms}$, $\Delta x = 0.1\text{cm}$ (stars, i.e. thick line), or $\Delta t = 0.01\text{ms}$, $\Delta x = 1\text{cm}$ (dotted line) both fail.	19
7	The implicit scheme (solid line) on the stretch- and stretch-rate-dependent contraction model described in (20), and the failure of the explicit scheme (stars, i.e. thick line) with the same model.	20

RECENT REPORTS

45/09	A Hybrid Radial Basis Function - Pseudospectral Method for Thermal Convection in a 3-D Spherical Shell	Wright Flyer
46/09	Refining self-propelled particle models for collective behaviour	Yates Baker Erban Maini
47/09	Stochastic Partial Differential Equations as priors in ensemble methods for solving inverse problems	Potsepaev Farmer Aziz
48/09	DiffUZZY: A fuzzy spectral clustering algorithm for complex data sets	Cominetti <i>et al.</i>
01/10	Fluctuations and instability in sedimentation	Guazzelli Hinch
02/10	Determining the equation of state of highly plasticised metals from boundary velocimetry	Hinch
03/10	Stability of bumps in piecewise smooth neural elds with nonlinear adaptation	Kilpatrick Bressloff
04/10	Random intermittent search and the tug-of-war model of motor-driven transport	Newby Bressloff
05/10	Ergodic directional switching in mobile insect groups	Escudero <i>et al.</i>
06/10	Derivation of a dual porosity model for the uptake of nutrients by root hairs	Zygalakis Roose
07/10	Frost heave in compressible soils	Majumdar Peppin Style Sander
08/10	A volume-preserving sharpening approach for the propagation of sharp phase boundaries in multiphase lattice Boltzmann simulations	Reis Dellar
09/10	Anticavitation and differential growth in elastic shells	Moulton Goriely
10/10	On the mechanical stability of growing arteries	Goriely Vandiver
11/10	Nonlinear Correction to the Euler Buckling Formula for Compressible Cylinders	De Pascalis Destrade Goriely

12/10	Nonlinear Morphoelastic Plates I: Genesis of Residual Stress	McMahon Goriely Tabor
13/10	Nonlinear Morphoelastic Plates II: Exodus to Buckled States	McMahon Goriely Tabor
14/10	Analysis of Brownian dynamics simulations of reversible biomolecular reactions	Lipkova Zygalakis Chapman Erban
15/10	Travelling waves in hyperbolic chemotaxis equations	Xue Hwang Painter Erban
16/10	The Physics and Mechanics of Biological Systems	Goriely Moulton
17/10	Crust formation in drying colloidal suspensions	Style Peppin
18/10	A Mathematical Model of Tumor-Immune Interactions	Robertson-Tessi El-Kareh Goriely
19/10	Elastic cavitation, tube hollowing, and differential growth in plants and biological tissues	Goriely Moulton Vandiver
20/10	Asymptotic expressions for the nearest and furthest dislocations in a pile-up against a grain boundary	Hall

Copies of these, and any other OCCAM reports can be obtained from:

**Oxford Centre for Collaborative Applied Mathematics
Mathematical Institute
24 - 29 St Giles'
Oxford
OX1 3LB
England
www.maths.ox.ac.uk/occam**